Food & Function

ROYAL SOCIETY OF CHEMISTRY

PAPER

View Article Online
View Journal | View Issue

Cite this: *Food Funct.*, 2024, **15**, 9176

An untargeted metabolomics approach applied to the study of the bioavailability and metabolism of three different bioactive plant extracts in human blood samples†

María del Carmen Villegas-Aguilar, *[a] María de la Luz Cádiz Gurrea,[a] María Herranz-López,[b] Enrique Barrajón-Catalán,[b] David Arráez-Román,[a] Álvaro Fernández-Ochoa*‡[a] and Antonio Segura-Carretero‡[a]

Advances in the understanding of bioavailability and metabolism of bioactive compounds have been achieved primarily through targeted or semi-targeted metabolomics approaches using the hypothesis of potential metabolized compounds. The recent development of untargeted metabolomics approaches can present great advantages in this field, such as in the discovery of new metabolized compounds or to study the metabolism of compounds from multiple matrices simultaneously. Thus, this study proposes the use of an untargeted metabolomics strategy based on HPLC-ESI-QTOF-MS for the study of bioavailability and metabolism of bioactive compounds from different vegetal sources. Specifically, this study has been applied to plasma samples collected in an acute human intervention study using three matrices (*Hibiscus sabdariffa*, *Silybum marianum* and *Theobroma cacao*). This approach allowed the selection of those significant variables associated with exogenous metabolites derived from the consumption of bioactive compounds for their subsequent identification. As a result, 14, 25 and 3 potential metabolites associated with supplement intake were significantly detected in the plasma samples from volunteers who ingested the *H. sabdariffa* (HS), *S. marianum* (SM) and *T. cacao* (TC) extracts. Furthermore, T_{max} values have been computed for each detected compound. The results highlight the potential of untargeted metabolomics for rapid and comprehensive analysis when working with a wide range of exogenous metabolites from different plant sources in biological samples.

Received 1st April 2024,
Accepted 9th August 2024

DOI: 10.1039/d4fo01522c

rsc.li/food-function

1. Introduction

Traditionally, plant-rich diets have been characterised by reports of various health benefits in humans. A significant portion of the beneficial properties of plant sources are associated with bioactive phytochemical compounds such as phenolic compounds.[1] When bioactive phenolic compounds are consumed, these phytochemicals can be absorbed or metabolised by host and intestinal microbiota enzymes.[2] The complex mixture of resulting metabolites may contribute additively or synergistically to bioactivities and may explain their beneficial effects.[1]

Given that the biochemical mechanisms of action of phenolic compounds are related to disease prevention, it is essential to fully understand their bioavailability and metabolization reactions to know exactly which chemical structures reach the target organs and tissues. Typical transformations in such phenolic compounds often involve the elimination of sugar moieties, resulting in the generation of aglycones from the initial compounds.[3] Furthermore, these compounds can undergo phase I and II metabolic biotransformation in the liver. Primary phase I metabolic reactions involve oxidation and reduction, while phase II reactions include processes such as methylation, sulphation, or glucuronidation.[3]

The absorption, bioavailability and metabolism of ingested phenolic compounds in both human and animal is generally explored by applying targeted metabolomics approaches.[4–6] This methodological choice revolves around the systematic search in biological samples for specific predetermined metabolites based on the original composition of the bioactive

[a]*Department of Analytical Chemistry, University of Granada, 18071 Granada, Spain. E-mail: marivillegas@ugr.es, alvaroferochoa@ugr.es; Tel: +34 958240794*
[b]*Institute of Research, Development and Innovation in Biotechnology of Elche (IDiBE) and Molecular and Cell Biology Institute (IBMC), Miguel Hernández University (UMH), 03202 Elche, Spain*

†Electronic supplementary information (ESI) available. See DOI: https://doi.org/10.1039/d4fo01522c

‡These authors shared author co-senior ship.

extracts and their hypothesized metabolic transformations.[4] These targeted strategies allow both the identification and quantification of the main metabolites predicted for plant matrices in biological samples, as long as commercial standards are available. Therefore, these strategies require a detailed characterization of the original composition of the bioactive extracts. However, these strategies do not have the ability to detect unpredicted or non-preselected compounds, and therefore the existence of completely new metabolites could go undetected.[7] This limitation becomes particularly obvious in plant matrices where information about the metabolites in plasma or urine is scarce. In such cases, relying solely on targeted strategies might result in substantial loss of valuable information.[8] To address this limitation, untargeted metabolomics strategies are gaining attention. These approaches involve analysing the entire range of compounds present in the samples without predefining a list of targets. Although the initial hypothesis of an untargeted methods does not pursue quantification, they offer a valuable advantage considering that they can reveal previously unknown or unexpected metabolites.[6,9,10]

In this context, by employing untargeted metabolomics strategies, we can acquire a much broader list of exogenous metabolites derived from the ingested extracts. Similarly, it enables the resolution of the issue of identifying metabolites originating from matrices with limited metabolomic studies.[9,10] Moreover, these untargeted strategies possess an added advantage in their potential application in multi-matrix studies. They allow rapid detection of circulating metabolites from various extracts without requiring prior knowledge of the original composition of the extract or the hypothesis of possible circulating metabolites. Considering all these aspects, this study proposes the application of an untargeted metabolomics-based study to study the bioavailability and metabolism of three extracts with different phenolic composition (*Hibiscus sabdariffa*, *Silybum marianum*, and *Theobroma cacao*).

H. sabdariffa, *S. marianum*, and *T. cacao* are three plant sources that have traditionally been employed for human consumption because of their reported beneficial properties.[1] Traditionally, these three plant sources have been consumed in different formats: *H. sabdariffa* (HS) in the form of infusions,[11] *S. marianum* (SM) as pharmaceutical preparations[12] and *T. cacao* (TC) in the form of chocolate and all its variations.[13]

The phenolic compounds present in the original extracts of these three plants have been widely studied by the scientific community. However, there are hardly any studies focused on the bioavailability and metabolism of these three plant matrices. Moreover, these three plants present different phenolic composition[14] allowing to cover the bioavailability and metabolism of different families of compounds through the application of this study.

Considering all the context, this study proposes an untargeted metabolomics methodology for the study of the bioavailability and metabolism of different bioactive extracts simultaneously. For its application, a case study is presented based on an acute intervention in humans where HS, TC and SM extracts were administered, and blood samples were collected at different times after the intake.

2. Experimental

2.1 Chemicals

All solvents employed in the analysis of metabolites were of analytical reagent grade and utilized in their original state. LC-MS grade methanol, water and formic acid, utilized as mobile phase components, were procured from Sigma-Aldrich (Steinheim, Germany). For plasma treatment, ethanol and methanol of LC-MS grade were sourced from Fisher Scientific (Madrid, Spain). The chemical standards used were Hibiscus Acid from Phytolab (Vestenbergsgreuth, Germany) and Quercetin-3 glucuronide from Sigma-Aldrich (St Louis, MO, USA).

2.2 Bioactive plant extracts

The HS, TC and SM extracts selected for the present study were pre-industrial extracts of the three plant matrices provided by NATAC Biotech S.L. (Cáceres, Spain). The extraction parameters were optimised for each plant matrix individually. For HS and TC extracts, a solid–liquid extraction (maceration) was performed using an EtOH : H_2O mixture (80 : 20; v : v) for two hours with a solvent : plant ratio of 20 : 1. For the SM extract a maceration was also performed but using an EtOH : H_2O mixture (96 : 4; v : v) for two hours with a solvent : plant ratio of 25 : 1. Extraction temperatures were set at 45 °C for HS, and 55 °C for SM and TC. The extracts obtained were dried under vacuum, stored at room temperature and protected from light until encapsulation. HS, SM and TC extracts at 5000 mg L^{-1} were characterised by high-performance liquid chromatography (Agilent 1290 HPLC, Agilent Technologies, Palo Alto, CA, USA) coupled to mass spectrometry with a quadrupole time-of-flight analyser (Agilent 6545 QTOF Ultra High Definition, Agilent Technologies, Palo Alto, CA, USA) using the methodology carried out in the previous study by Villegas-Aguilar *et al.* (2024).[14]

2.3 Biological samples

The study protocol adhered to the ethical recommendations of the Declaration of Helsinki and received approval from the Ethics Committee of the Miguel Hernández University of Elche and the Universitary Hospital of Elche (Alicante, Spain), reference PI 57/2019. The study involved 33 healthy subjects with a mean age and body mass index of 27 ± 9 years and 23 ± 3 kg m^{-2}, respectively. Participants were not taking medication or nutritional supplements and did not have any chronic pathology or gastrointestinal disorder. The sample size was estimated based on similar previous bioavailability studies.[4] Volunteers provided informed consent before participating.

The study was conducted at the facilities of Universidad Miguel Hernández. After an overnight fast, volunteers were divided into three groups: 8 consumed an encapsulated (pill) 500 mg *H. sabdariffa* calyxes extract, 8 consumed an encapsu-

lated (pill) 500 mg *S. marianum* fruit extract, 8 consumed an encapsulated (pill) 500 mg *T. cacao* fruit extract and 9 consumed an encapsulated (pill) placebo. A polyphenol-free breakfast was offered 30 minutes after encapsulation consumption, and at 2.5, 4.5, and 9.5 hours after ingestion, a polyphenol-free snack and lunch were provided. Water was available *ad libitum*.

Before encapsulation ingestion, a nurse inserted a cannula into the ulnar vein of the non-preferred arm of the volunteers. Blood samples were collected in EDTA-coated tubes at baseline ($t = 0$) and subsequently at 0.5, 1, 2, 4, 6, 8, and 10 hours after encapsulation consumption. Plasma was separated by centrifugation (10 min, 3000 rpm, 4 °C) and stored at −80 °C until further analysis.

2.4 Sample treatment

The plasma samples, preserved at −80 °C until analysis, were initially thawed on ice. For sample processing, a 100 µl plasma aliquot was blended with 200 µl of methanol : ethanol (50 : 50, v/v). Following a 10 second vertexing, the mixture was maintained at −20 °C for 30 minutes to facilitate sufficient protein precipitation. Subsequently, the sample underwent centrifugation for 10 minutes at 14 000 rpm and 4 °C. The resulting supernatant was subjected to a 2 hour vacuum evaporation in a centrifugal evaporator (Concentrator Plus, Eppendorf, Hamburg, Germany). The reconstituted residue was dissolved in 80 µl of the initial mobile phase conditions (0.1% aqueous formic acid : methanol, 95 : 5, v/v). Finally, a 60 µl aliquot was transferred to an HPLC vial and stored at −80 °C until the day of analysis. A quality control (QC) sample was prepared by combining equal volumes (20 µl) from each original sample. Multiple QC aliquots were processed following the same methodology as described for the samples.

2.5 HPLC-ESI-QTOF-MS analysis

The analyses were conducted in an Agilent 1260 HPLC instrument (Agilent Technologies, Palo Alto, CA, USA) coupled to an Agilent 6540 Ultra High Definition (UHD) Accurate Mass Q-TOF, equipped with a dual Jet Stream ESI† interface. A reversed-phase analytical C18 column (Agilent Zorbax Eclipse Plus, 1.8 µm, 4.6 × 150 mm) with a protective cartridge of the same packing was employed. The mobile phases included water with 0.1% formic acid (mobile phase A) and methanol (mobile phase B). To ensure effective separation, a gradient of these mobile phases was applied as follows: 0 min [A : B, 95/5], 5 min [A : B, 90/10], 15 min [A : B, 15/85], 30 min [A : B, 5/95], and 35–40 min [A : B, 95/5]. The column and autosampler compartment temperatures were maintained at 25 and 4 °C, respectively. The injection volume and flow rate were set at 2.5 µl and 0.4 ml min^{-1}.

Detection was performed in negative ion mode within the range of 50 to 1700 *m*/*z*. All spectra underwent correction *via* continuous infusion of two reference masses: TFA anion (*m*/*z* 112.985587) and HP-921 (*m*/*z* 1033.988109). Both reference ions provided accurate mass measurements, typically better than 2 ppm.

Ultrapure nitrogen and a nebulizer served as drying and nebulizing gas at temperatures of 200 and 350 °C, with flow rates of 10 and 12 L min^{-1}, respectively. Other optimised parameters were as follows: fragmentor, 130 V; capillary voltage, +4000 V; nebuliser, 20 psi; nozzle voltage, 500 V; skimmer, 45 V and octopole 1 RF Vpp, 750 V.

The sequence design has been carried out according to the guidelines and considerations established in untargeted metabolomics studies.[15] For sample analysis, analytical blanks were analysed at the beginning and at the end of the sequence. Quality control samples were analysed at the beginning of the sequence, after the first blanks, to stabilize instrumental conditions. Additionally, QCs were also injected throughout the entire sequence, every 6 real samples, to ensure analytical reproducibility. Samples from different groups (placebo or different supplements) were randomised in the sequences, but different samples from the same volunteer were analysed consecutively. Finally, targeted MS/MS analyses were performed on the signals of interest to obtain a fragmentation spectrum for metabolite annotation. This experiment was performed using nitrogen as collision gas with the following collision energies: 10 eV, 30 eV and 60 eV.

2.6 Data processing

Firstly, the raw data (.d format) acquired by HPLC-ESI-QTOF-MS were converted to .mzML format using the data processing tool Msconvert (ProteoWizard). MZmine 3.9.0 software was used to run several data preprocessing stages including mass detection, chromatogram builder, deconvolution, alignment, isotopic grouping and duplicate peak filter. The following parameters were optimized and selected to carry out the different data processing stages. For the mass detection stage, a noise level of 3.0E2 was selected. The construction of chromatograms was based on the ADAP algorithm selecting the following parameters: intensity threshold: 3.0E2; highest minimum intensity: 1.E3; *m*/*z* tolerance: 20 ppm. For chromatogram deconvolution, the wavelet algorithm (ADAP) was applied with the following parameters: S/N threshold of 10, minimum peak height of 6.0E2, coefficient/area threshold of 110, peak duration range from 0.00 to 10.00, and RT wavelet width range from 0.00 to 0.10. Chromatogram alignment was conducted using the "Join Aligner" algorithm, with an *m*/*z* tolerance of 15 ppm and an RT tolerance of 0.25 min, assigning equal weight to both *m*/*z* and RT. Finally, the duplicate peak filter stage was implemented with a selected *m*/*z* tolerance of 15 ppm and a retention time tolerance of 0.1 min.

The following data processing steps were conducted using an open-source methodology through a combination of different R packages.[16] For the batch normalization step, missing values (NAs) were imputed by a small value. The batchCorr (v 0.2.5.) package was used to correct the signal intensity drift between and within batches.[17] The imputed NAs were subsequently converted back to NAs after batch normalization. Notame R package was mainly used to filter biologically meaningless signals such as potential contaminants or low

detected signals. Thus, the *flag_contaminants* function was used to filter out those molecular features considered as contaminants since they were also detected in blank samples. The *flag_detection* function was also run to exclude the molecular features with low detection rates for the study groups. A flag detection threshold of 0.5 was chosen for filter out those signals with low detection in the analysed samples. 8 groups were established for each matrix according to the different sample collection times (0, 0.5, 1, 2, 4, 6, 8 and 10 hours). Therefore, all those signals that were not detected in 50% of the volunteers in at least one of these subgroups were filtered. For this filter, all chromatographic areas less than 80 counts were considered NAs since those integrated values are below the noise level.

2.7 Statistical analysis

Statistical analyses were aimed at selecting those variables associated with the intake of bioactive supplements, which are related to bioavailable and/or metabolized compounds. For this objective, a combination of univariate and multivariate statistical analyses was applied to the pre-processed dataset. All statistical analyses were run using MetaboAnalyst 6.0 software. Prior to conducting multivariate analyses, the data were logarithmic transformed, and Pareto scaled. These measures aimed to normalize the data and mitigate the impact of variables with large scales.

Firstly, a Principal Component Analysis (PCA) was performed to assess reproducibility, check data quality and identify potential outliers. A hierarchical clustering analysis was conducted through a heatmap, providing a preliminary visual representation of the data based on the different experimental groups. For those analyses, the variables with a relative standard deviation (RSD) higher than 30% in QC samples were also filtered out.

Finally, the following criteria was used to select the potential molecular features related to exogenous metabolites of the extract for subsequent identification:

- Molecular features do not have to be identified as contaminants based on the flag contaminant function.

- Molecular features have to be detected in at least 50% of one of the subgroups, excluding time 0, of the volunteers who consumed the extracts. On the contrary, molecular features do not have to be detected in the subgroups of the volunteers who consumed the placebo supplement.

- The molecular features do not have to be detected at the time 0 subgroups.

The time to reach maximum concentration (T_{max}) was calculated for each significant metabolite was calculated using PKSolver, an add-in program for pharmacokinetic dana analysis in Microsoft Excel.[18]

2.8 Metabolite identification

The metabolite identification of selected molecular features was conducted by comparing the acquired accurate mass, isotopic distribution, and fragmentation spectra derived from MS/MS analysis with information available in comprehensive metabolomic databases. The metabolite annotation step was facilitated by and the CEU Mass Mediator tool, a versatile resource developed by Gil de la Fuente *et al.* (2018).[19] This tool enabled simultaneous exploration of multiple databases, including METLIN, LipidMaps, and the Human Metabolome Database.

Furthermore, to enhance the accuracy of our identifications, MS/MS patterns were cross-referenced with *in silico* MS/MS fragmentation resources, specifically using SciFinder®, Sirius 5.8.5 and MetFrag (**https://ipb-halle.github.io/MetFrag/**).

According to the identification guidelines proposed by Sumner *et al.* (2007),[20] compounds were annotated at level 1 with commercial standards, at level 2 by comparing the MS/MS spectra with those present in the databases, at level 3 based on the molecular formulation and MS1 spectra and at level 4 where the molecules remain as unknowns.

3 Results and discussion

3.1 Phytochemical composition of *Hibiscus sabdariffa*, *Silybum marianum* and *Theobroma cacao* extracts

The detailed phytochemical characterization of HS, SM and TC extracts is reported in Tables S1–S3 (ESI†), respectively.

In summary, 40 compounds were annotated in the HS extract, including a high presence of hibiscus acid, hibiscus acid lactone, and its methylated forms and glycosylated flavonoids, such as quercetin 3-*O*-rutinoside and quercetin 7-glucoside.

In the SM extract, a total of 67 compounds were tentatively identified. Notably, there was a high content of flavolignans, with prominent compounds including silybin and its isomers such as silychrystin, isosilybin B, as well as modified forms like dehydrosilybin, hydrogenated silybin, and acetylsilybin A/B. Additionally, the extract contained other flavonoids such as taxifolin (dihydroquercetin).

Finally, 53 compounds were annotated in the TC extract, quinic acid and gluconic acid being the main compounds present. Additionally, the presence of vanillic acid was noteworthy in this extract.

Consequently, the phenolic content varies significantly among these three matrices, showcasing a diverse array of phenolic compounds from various families. Hence, these three matrices were chosen for the implementation of untargeted metabolomics methodology in bioavailability and metabolism studies. One of the key advantages of employing untargeted methodology is its versatility and therefore in multi-matrix studies makes it unnecessary to hypothesize beforehand all potential metabolization reactions.

In addition, total phenolic content was measured by the Folin–Ciocalteu method using gallic acid as the reference compound for the standard curve of the extracts of HS, SM and TC used in the acute intervention study in the previous study by Villegas-Aguilar *et al.* (2024).[14] The total phenolic content values obtained were 51 ± 1, 617 ± 8, and 255 ± 12 mg gallic acid equivalent per g dry extract for HS, SM,

and TC, respectively. Therefore, it is evident that SM exhibits a higher total phenolic content compared to the other two extracts.

3.2 Untargeted metabolomic data analysis for the study of bioavailability and metabolism of bioactive compounds of the three bioactive extracts

After data processing with MZmine 3.9.0 software, a data matrix consisting of 22 598 molecular features was obtained. Subsequently, the various filtering steps mentioned in the Experimental section (*e.g.* potential contaminants, low presence signals, *etc.*), resulting in a refined data matrix containing 6360 molecular features. These molecular features correspond to potential compounds that are present in at least half of the individuals in the defined subgroups (*i.e.*, one subgroup per matrix and collection time), including the time 0 and placebo subgroups. This dataset based on the 6360 molecular features was subjected to the different statistical analyses. Additionally, to check data quality, the molecular features with a relative standard deviation (RSD) higher than 30% in QC samples were filtered out. Following this filter, 5328 molecular features were finally selected for further analysis.

To assess data quality after applying the selected parameters, an initial overview of the performance quality was obtained through PCA of the entire dataset, including all QC samples (Fig. 1). The PCA reveals well-clustered QC samples, indicating good data quality. Regarding the remaining samples, it is notable that the SM samples, in particular, exhibit the most distinct separation from the placebo samples. This subset of differentiated SM samples showed lower scores in the PC1 and higher scores in the PC3 with respect to the rest of biological samples. This deviation of a significant percentage of samples from the SM group from the rest of the samples in the PCA score analysis is indicative of the presence of upregulated signals in these SM samples, which may be associated with the intake of the bioactive SM supplement. This highlights that PCA analysis can offer a first overview of the data, revealing the data quality as well as the relevance of potential exogenous metabolites in the datasets. In addition, additional PCA analysis were performed considering data from

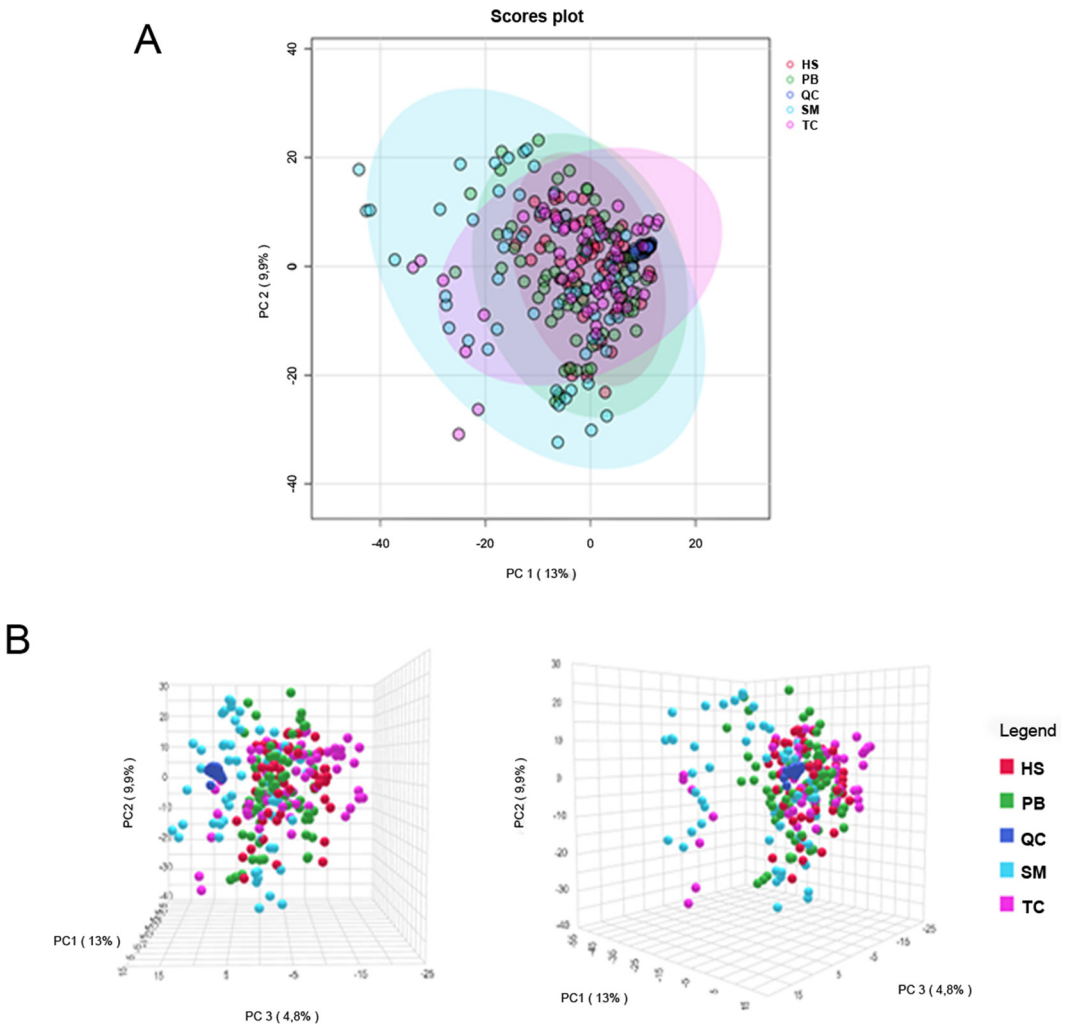

Fig. 1 (A) 2D PCA scores plots from normalized data for plasma samples. (B) 3D PCA scores plots from normalized data for plasma samples.

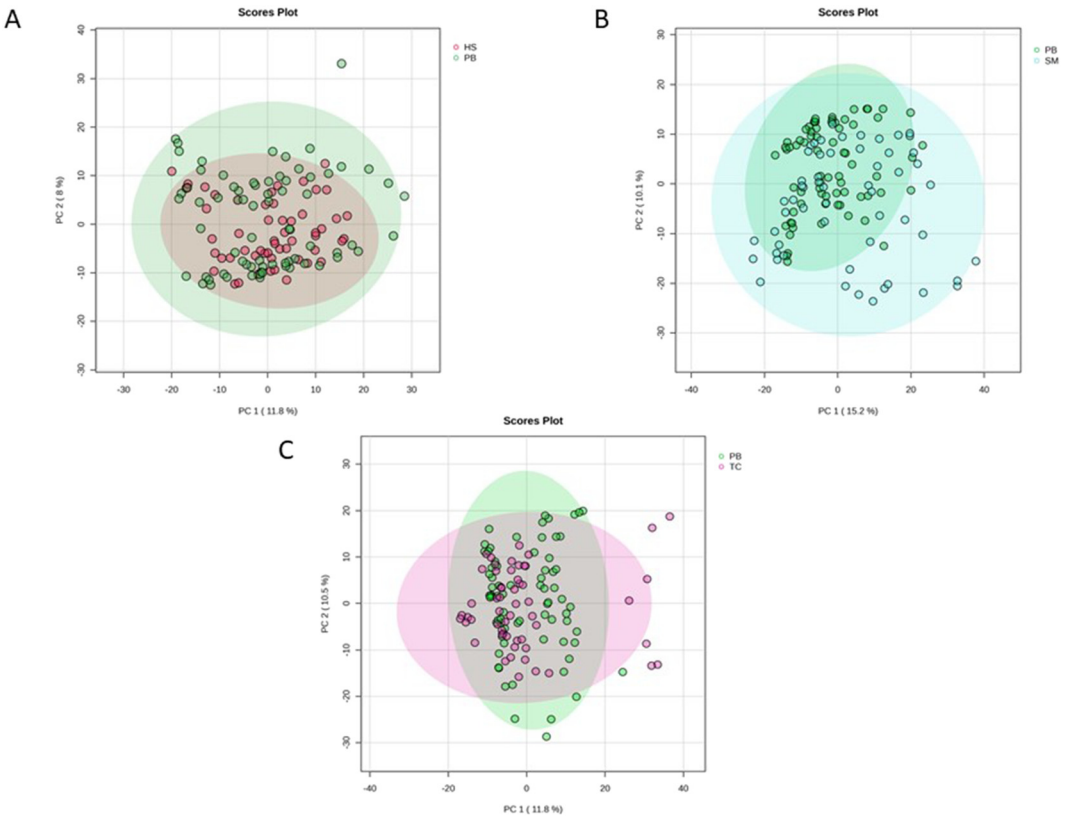

Fig. 2 (A) 2D PCA scores plots from normalized data for plasma samples from *H. sabdariffa* and placebo. (B) 2D PCA scores plots from normalized data for plasma samples from *S. marianum* and placebo. (C) 2D PCA scores plots from normalized data for plasma samples from *T. cacao* and placebo.

the placebo group and each of the supplement groups (HS, SM, and TC) but separately (Fig. 2). Similar trends are observed with respect to the global PCA (Fig. 1) since there is a subset of SM samples separated from the placebos through high scores values at PC1 and low values at PC2 (Fig. 2B). However, in the case of all TC and HS samples, a general overlap of almost all studied samples is observed with the placebo samples (Fig. 2A and C).

The subsequent step involves filtering those molecular features detected in the placebo samples as well as in the plasma samples collected at time 0 before the intake of the supplements. After applying the filter, a matrix with 85 molecular features was generated, and a hierarchical clustering analysis *via* heatmap considering those signals was generated (Fig. 3). In this heatmap, samples collected at time 0 in the experimental groups were not considered for averaging the signals in those groups. Therefore, the rest of samples collected at 0.5, 1, 2, 4, 6, 8, and 10 hours were used for this analysis. In this heatmap, it is evident the presence of three different clusters that each one of them is associated with a different matrix, highlighting the difference in size in terms of the number of signals in each one of them, the most numerous being the SM cluster, then the HS cluster, and finally the smallest being the TC cluster.

The interactive heatmap allows users to visualise broad multidimensional results from untargeted metabolomics and identify significantly altered features by customising the visualisation.[21] These results illustrate the swift acquisition of such plots once the filtering criteria are established, enabling the prompt identification of signals linked to supplement intake. Moreover, it is worth noting the considerable variances in the number of biomarkers associated with intake across the different matrices in this study. These distinctions may primarily arise from variances in the richness of the original extract compositions or the bioavailability of phenolic compounds within each matrix. Significantly, certain phenolic compounds exhibit higher bioavailability than others. For instance, based on the literature isoflavones compounds are the most bioavailable followed by phenolic acids, flavanols, flavanones, and flavonols, and the least bioavailable are anthocyanins and proanthocyanidins.[22]

The analysis carried out prior to the identification using statistical analysis can be highly beneficial when analysing this type of data involving exogenous metabolites from different plant samples. In this regard, the results of the heatmaps revealed that there are no compounds in common between the three matrices, a finding that has been corroborated by identifying the molecular features. Additionally, the heatmaps predicted that the SM matrix has the widest variety of compounds, a conclusion further supported by the identification process,

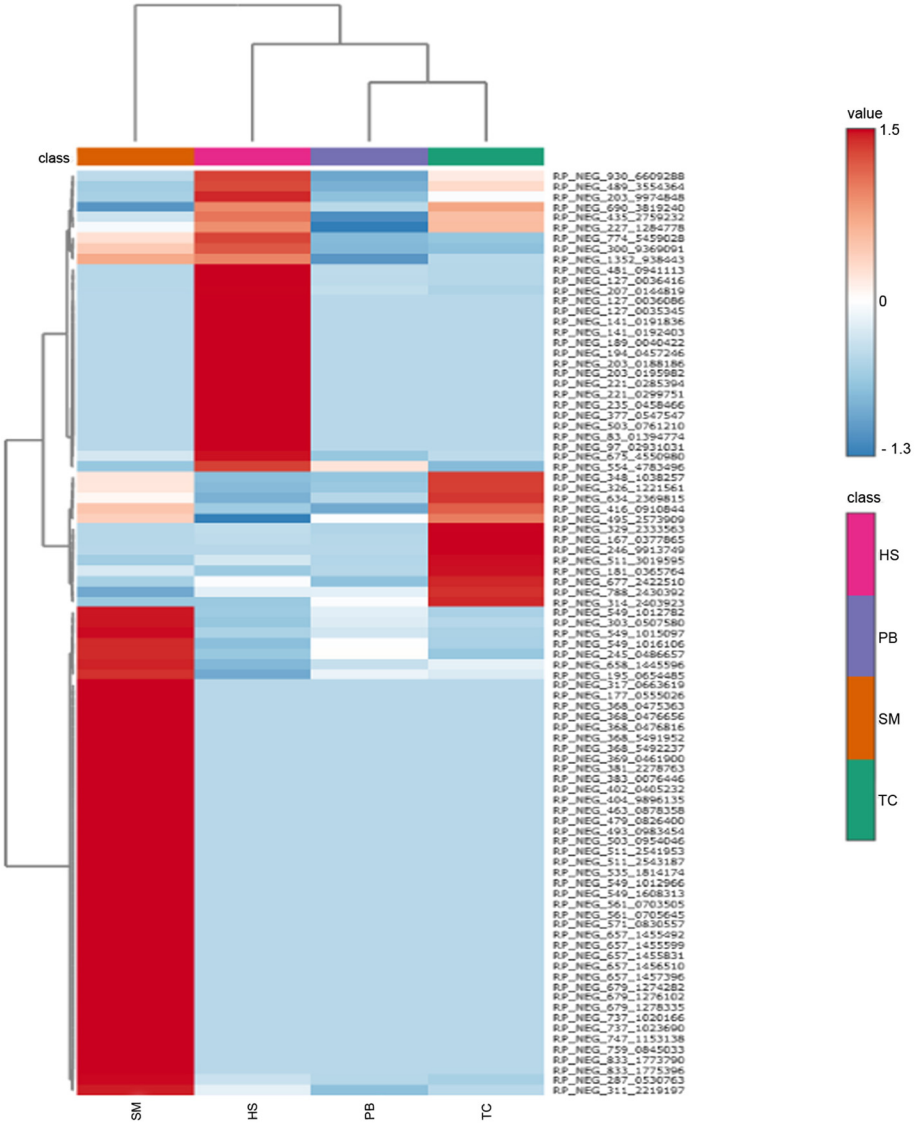

Fig. 3 Hierarchical clustering analysis by heat map using the areas under the curve of the 85 characteristic molecules selected for plasma from the three matrices.

while highlighting the scarcity of metabolites present in plasma after TC intake.

After analysing these findings, a heatmap analysis was conducted, categorizing the selected metabolites in plasma from the three matrices by group and time (Fig. 4) to assess whether this graphical representation enables us to discern the times at which the metabolites appear for each type of ingested sample. Indeed, as indicated by the calculated T_{max}, it is observed that for the metabolites from HS, there is a prevailing trend for most of them to appear at a time very close to 1–2 hours after ingestion of the extract. Conversely, for the metabolites resulting from the ingestion of SM, there is a subset of compounds with a T_{max} of approximately one hour, while others exhibit a T_{max} of around 3 hours.

This heatmap offers a wealth of information surpassing that of the previous one depicted (Fig. 3), as it disaggregates the groups according to their respective time points.

3.3 Identification of significant signals related to supplement intake

After applying the criteria for selecting significant signals associated with supplement intake using an untargeted metabolomic approach, a total of 85 compounds were proposed as exogenous metabolites present in plasma following extract ingestion. Finally, 25, 14 and 3 compounds were annotated in the volunteers who consumed SM, HS and TC, respectively. 43 molecular features could not be annotated and were kept as unknown compounds (Table S4†).

In addition, T_{max} values have been calculated for each compound detected.

For greater detail of the bioavailable and metabolized compounds detected in plasma samples, the subsections focus on describing these results for each of the studied vegetal matrix.

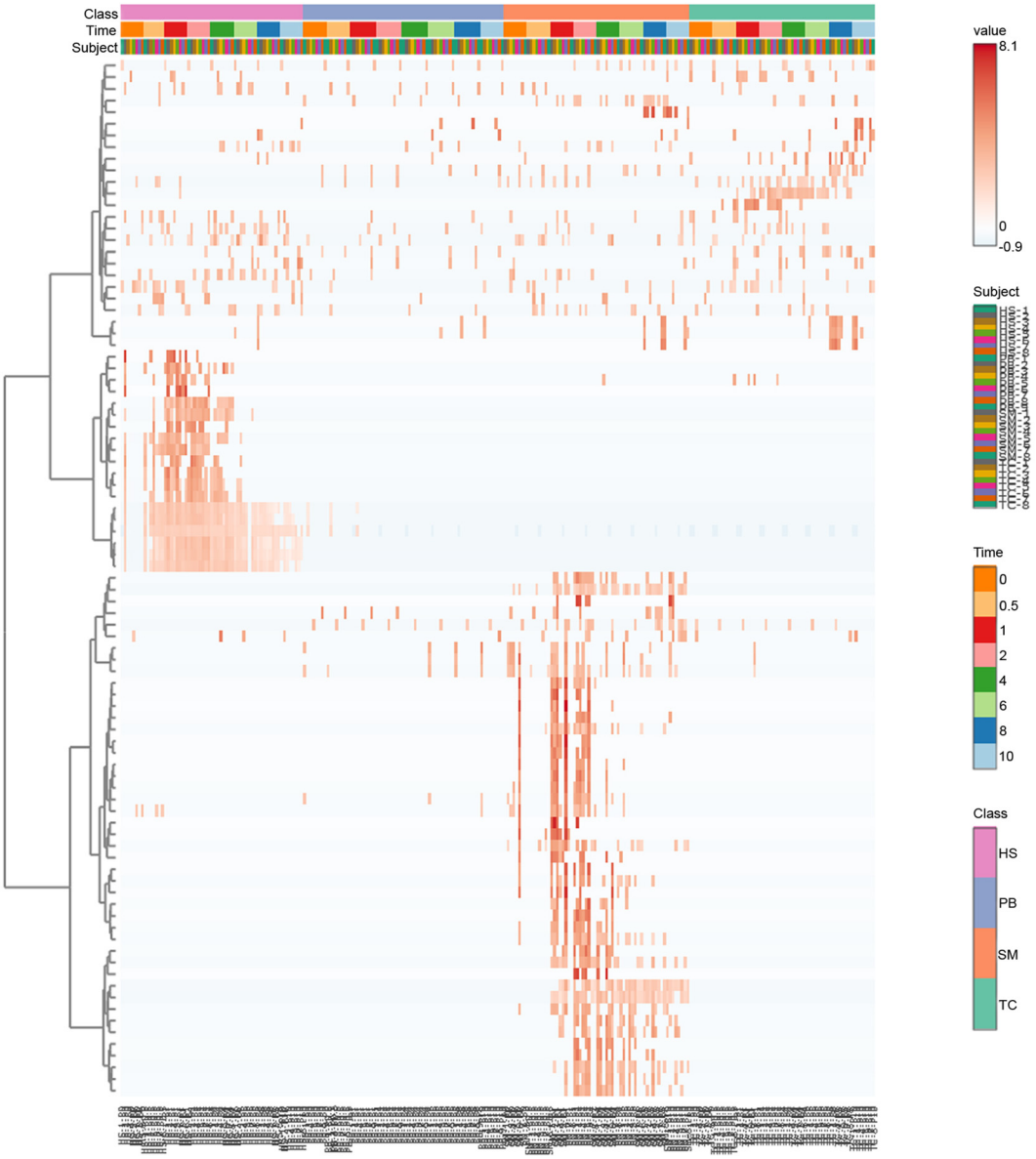

Fig. 4 Hierarchical clustering analysis by heat map using the areas under the curve of the selected metabolites in plasma from the three matrices by group and time.

3.3.1 Circulating metabolites detected in plasma related to the intake of *Hibiscus sabdariffa* extract. Table 1 lists the bioavailable metabolites detected in the plasma samples related to the intake of the *H. sabdariffa* extract supplement. In total, 14 compounds were annotated in volunteers who ingested the HS extract. Among the 14 compounds analysed, hydroxycitric acid lactone was identified by comparison with its commercial standard. Fig. S1† reports the MS/MS spectra of the analysed standard, which along with the retention time matched with the significant feature detected in the HS volunteers. Additionally, 10 compounds were annotated at level 2 by comparison of MS/MS spectra with those reported in databases, and 3 compounds at level 3. Consequently, approximately 79% of the annotated compounds were annotated at levels 1 and 2, indicating high annotation reliability. The remaining 21% of the compounds annotated at level 3 annotation are considered less accurate, although the supporting bibliographic data suggests a high likelihood of proper annotation.

When comparing the presence of metabolites in plasma with the content of the original extract as reported by Villegas-Aguilar *et al.* (2024),[14] it is evident that certain compounds pass into plasma without undergoing modification in their native form. Hence, compounds like hydroxycitric acid, hibiscus acid and two isomers of hibiscus acid monomethyl ester, which are characteristic constituents found in significant quantities in this plant matrix, enter the plasma directly without undergoing any alteration. In this sense, when these compounds enter the bloodstream, they can exhibit in target

Table 1 HPLC-ESI-QTOF-MS identification information and relative nutrikinetic parameters of the metabolites detected in plasma samples after intake of an extract of *H. sabdariffa*

Peak	RT (min)	Observed *m/z*	Adduct	Theoretical *m/z*	Mass error (ppm)	Molecular formula	Level of annotation	Proposed compound	MS/MS fragments	Ref.[a]	*n*	T_{max}
1	1.12	127.0035	$(M-H)^-$	127.0037	−1.16	$C_5H_4O_4$	2	5-Hydroxy-2-furoic acid isomer 1	85.0298; 55.0219	HMDB59784	7	1.43 ± 1.05
2	1.13	377.0548	$(M-H)^-$	377.0514	8.84	$C_{17}H_{14}O_{10}$	2	3,4,5-Trihydroxy-6-({7-oxo-7*H*-furo[3,2-*g*]chromen-4-yl}oxy)oxane-2-Carboxylic acid	300.006	HMDB0129424	7	1.43 ± 0.68
3	1.17	207.0157	$(M-H)^-$	207.0146	5.12	$C_6H_8O_8$	2	Hydroxycitric acid	127.0034; 87.0078; 189.0014	HMDB0031159	8	1.19 ± 0.50
4	1.19	481.0941	$(M-H)^-$	481.0988	−9.67	$C_{21}H_{22}O_{13}$	2	Epigallocatechin-7-glucuronide	313.0655; 191.0181	HMDB0041640	8	1.50 ± 0.50
5	1.23	127.0036	$(M-H)^-$	127.0037	−0.32	$C_5H_4O_4$	2	5-Hydroxy-2-furoic acid isomer 2	85.0298; 55.0221	HMDB59784	8	1.50 ± 0.50
6	1.43	221.0285	$(M-H)^-$	221.0303	−7.92	$C_7H_{10}O_8$	2	Methoxycitric acid isomer 1	127.0036; 189.0030	Pubchem: 44149934	8	1.88 ± 0.33
7	1.50	203.0188	$(M-H)^-$	203.0197	−4.47	$C_7H_8O_7$	3	Hibiscus acid monomethyl ester isomer 1	—	29	8	2.13 ± 1.17
8	2.02	203.0196	$(M-H)^-$	203.0197	−0.63	$C_7H_8O_7$	3	Hibiscus acid monomethyl ester isomer 2	—	29	8	1.63 ± 0.48
9	2.21	189.0040	$(M-H)^-$	189.0041	−0.31	$C_6H_6O_7$	1[b]	Hydroxycitric acid lactone (hibiscus acid)	127.0039; 87.0072; 111.0066; 57.0347	HMDB0259498	8	1.75 ± 0.43
10	2.22	221.0300	$(M-H)^-$	221.0303	−1.43	$C_7H_{10}O_8$	2	Methoxycitric acid isomer 2	127.0029; 189.0023	Pubchem: 44149934	8	1.75 ± 0.43
11	2.22	127.0036	$(M-H)^-$	127.0037	−0.58	$C_5H_4O_4$	2	5-Hydroxy-2-furoic acid isomer 3	85.0298; 55.0220	HMDB59784	8	1.75 ± 0.43
12	5.45	97.0293	$(M-H)^-$	97.0295	−1.99	$C_5H_6O_2$	3	2-Furanmethanol	—	28		1.00 ± 0.00
13	6.27	235.0458	$(M-H)^-$	235.0459	−0.40	$C_8H_{12}O_8$	2	Hibiscus acid hydroxyethylester	127.0032	30	8	1.50 ± 0.50
14	11.87	194.0457	$(M-H)^-$	194.0432	13.01	$C_6H_{11}O_7$	2	D-Gluconate	151.1002	29	5	0.90 ± 0.20
Average												1.52 ± 0.32

n: number of volunteers in whom the metabolite appears after ingestion of the *H. sabdariffa* encapsulate; RT: retention time; T_{max}: time required to reach the relative maximum plasma level (h); values represent mean ± standard deviation (*n* = number of volunteers in whom the metabolite appears). [a] Database or bibliography used for compound annotation. [b] Mass fragmentation spectrum of the analytical standard in Fig. S1.†

cells their bioactivity demonstrated *in vivo* in several studies, such as the antimicrobial and anti-diabetic power of hibiscus acid and the antioxidant and anti-inflammatory power demonstrated for hydroxycitric acid.[23]

Other compounds detected in the plasma were not originally present in the extract but are metabolized derivatives of compounds characterised in it. Hence, for instance, hibiscus acid hydroxyethylester may have been generated in plasma upon the addition in hibiscus acid of a methyl group and a hydroxyl group to the methyl ester group. Therefore, these compounds undergo both phase I and phase II metabolic reactions. Methylation of this group can occur *via* catechol-*O*-methyltransferases in the liver, small intestine or kidneys, with the liver being the primary site.[24]

Also noteworthy is the presence in plasma of two isomers of methoxycitric acid, compounds that were not found in the original extract but may owe their presence in plasma to the methylation of hydroxycitric acid, which was characterized in the extract and in plasma.

It should be noted that most of the compounds detected in plasma after ingestion of the HS extract exhibit a T_{max} between 1 and 2 hours. When compared with the T_{max} values obtained in the study conducted by Arce-Reynoso *et al.* (2023),[25] where a *H. sabdariffa* drink containing compounds such as hibiscus acid and hydroxycitric acid were also detected in plasma but with T_{max} values of 2.7 ± 1.2 and 2.5 ± 2.34 hours, respectively, our study shows earlier T_{max} values of 1.75 ± 0.43 and 1.19 ± 0.50 hours for these same compounds. The earlier T_{max} values observed in our study could be attributed to differences may be related to the format of the product (beverage *vs.* capsule). However, in accordance with the findings of these authors, the low T_{max} values are indicative of intestinal absorption of the compounds.[25]

The detection of 5-hydroxy-2-furoic acid in the extract is likely attributable to the presence of vitamin C (ascorbic acid). While our methodology, designed for the identification of phenolic compounds, cannot directly detect vitamin C, existing literature supports a high ascorbic acid content in the source material (HS).[26] Ascorbic acid oxidation leads to dehydroascorbic acid, a known precursor to 5-hydroxy-2-furoic acid through subsequent hydroxylation *via* metabolic pathways.[27]

In the case of the compounds annotated as D-gluconate and 2-furanmethanol, their presence in plasma is justified by previous reports of these compounds in HS extract.[28,29]

3.3.2 Circulating metabolites detected in plasma related to the intake of *Silybum marianum* extract. Table 2 presents a comprehensive list of 25 metabolites annotated in plasma through an untargeted metabolomics approach in volunteers who consumed *S. marianum* extract. Among the 25 compounds, quercetin glucuronide was identified by comparison with its analytical standard (Fig. S2†). 22 molecular features were annotated at level 2 annotation (comparison of MS/MS spectra), and 2 at level 3 (based on molecular mass and literature search). Consequently, approximately 92% of the annotated compounds achieved at least level 2 of annotation, indicating high annotation reliability.

Table 2 HPLC-ESI-QTOF-MS identification information and relative nutrikinetic parameters of the metabolites detected in plasma samples after intake of an extract of *S. marianum*

Peak	RT (min)	Observed *m/z*	Adduct	Theoretical *m/z*	Mass error (ppm)	Molecular formula	Level of annotation	Proposed compound	MS/MS fragments	Ref.[a]	*n*	T_{max}
1	11.55	463.0878	$(M-H)^-$	463.0882	−0.79	$C_{21}H_{20}O_{12}$	2	Myricetin rhamnoside	195.8083	34	4	1.00 ± 0.00
2	11.64	493.0983	$(M-H)^-$	493.0988	−0.85	$C_{22}H_{22}O_{13}$	2	Methyl taxifolin glucuronide	317.0665; 195.8111	35	6	1.33 ± 0.47
3	12.02	369.0462	$(M-H)^-$	369.0463	−0.39	$C_{15}H_{14}O_{11}$	2	Caffeoylhydroxycitric acid	191.0232;135.0456	Pubchem: 24797519	6	1.00 ± 0.00
4	13.02	737.1020	$(M-H)^-$	737.1029	−1.23	$C_{31}H_{30}O_{19}S$	2	Silybin sulphate glucuronide isomer 1	561.0701; 481.1215; 325.0723	—	6	2.17 ± 0.90
5	13.22	383.0076	$(M-H)^-$	383.0078	−0.51	$C_{15}H_{12}O_{10}S$	2	Taxifolin sulphate	125.0945	36	8	1.25 ± 0.43
6	13.32	657.1457	$(M-H)^-$	657.1461	−0.70	$C_{31}H_{30}O_{16}$	2	Silybin glucuronide isomer 1	481.1150; 301.0309; 113.0227	37	4	8.50 ± 0.87
7	13.33	477.0649	$(M-H)^-$	477.0675	−5.45	$C_{21}H_{18}O_{13}$	1[b]	Quercetin glucuronide	301.0348; 151.0044; 178.9993; 113.0248	HMDB0029212	6	1.33 ± 0.47
8	13.46	737.1024	$(M-H)^-$	737.1029	−0.75	$C_{31}H_{30}O_{19}S$	2	Silybin sulphate glucuronide isomer 2	561.0701; 481.1215; 325.0724	—	7	4.00 ± 2.62
9	13.48	303.0508	$(M-H)^-$	303.0510	−0.88	$C_{15}H_{12}O_7$	2	Taxifolin (dihydroquercetin)	125.0953	HMDB0303943	6	2.42 ± 2.54
10	13.72	657.1457	$(M-H)^-$	657.1461	−0.56	$C_{31}H_{30}O_{16}$	2	Silybin glucuronide isomer 2	481.1150; 113.0224; 301.0309;	37	8	1.38 ± 0.48
11	13.84	679.1274	$(M-H)^-$	679.1305	−4.46	$C_{33}H_{28}O_{16}$	2	Silybin 3,23-bishemisuccinate isomer 1	551.6985; 116.9318; 262.9476	38	7	2.43 ± 2.32
12	13.98	657.1456	$(M-H)^-$	657.1461	−0.83	$C_{31}H_{30}O_{16}$	2	Silybin glucuronide isomer 3	481.1150; 113.0224; 301.0309;	37	7	4.38 ± 2.34
13	14.16	195.0654	$(M-H)^-$	195.0663	−4.27	$C_{10}H_{12}O_4$	2	Xanthoxylin	160.8413	Pubchem ID: 66654	5	4.60 ± 4.41
14	14.27	657.1455	$(M-H)^-$	657.1461	−0.85	$C_{31}H_{30}O_{16}$	2	Silybin glucuronide isomer 4	481.1150; 113.0224; 301.0309; 113.0224	37	6	1.42 ± 1.17
15	14.34	317.0664	$(M-H)^-$	317.0667	−0.99	$C_{16}H_{14}O_7$	2	Methyltaxifolin	187.0063; 125.0217	35	6	1.17 ± 0.37
16	14.38	287.0531	$(M-H)^-$	287.0561	−10.58	$C_{15}H_{12}O_6$	2	Eriodictyol	251.1362	Pubchem ID: 440735	6	1.25 ± 0.56
17	14.73	679.1276	$(M-H)^-$	679.1305	−4.19	$C_{33}H_{28}O_{16}$	2	Silybin 3,23-bishemisuccinate isomer 2	551.6985; 116.9318; 262.9477	38	5	2.20 ± 0.98
18	14.75	657.1456	$(M-H)^-$	657.1461	−0.80	$C_{31}H_{30}O_{16}$	2	Silybin glucuronide isomer 5	481.1150; 113.0224; 301.0309; 113.0226	37	5	1.80 ± 1.17
19	14.91	561.0704	$(M-H)^-$	561.0708	−0.86	$C_{25}H_{22}O_{13}S$	2	Silybin sulphate isomer 1	481.1130; 455.1290; 367.1237; 125.0237	37	6	2.17 ± 0.90
20	14.93	679.1278	$(M-H)^-$	679.1305	−3.86	$C_{33}H_{28}O_{16}$	2	Silybin 3,23-bishemisuccinate isomer 3	551.6985; 116.9318; 262.9478	38	4	1.75 ± 0.43
21	15.12	561.0706	$(M-H)^-$	561.0708	−0.48	$C_{25}H_{22}O_{13}S$	2	Silybin sulphate isomer 2	481.1130; 455.1290; 367.1237; 125.0238	37	7	3.14 ± 2.10
22	15.59	571.0831	$(M-H)^-$	571.0882	−9.01	$C_{30}H_{20}O_{12}$	3	2,3-Dihydro-5′,3″′-dihydroxyamentoflavone	—	C00006510	5	1.20 ± 0.40
23	16.73	381.2279	$(M-H)^-$	381.2283	−1.01	$C_{21}H_{34}O_6$	3	Sarcostin	—	Pubchem ID: 46173994	6	1.33 ± 0.47
24	17.27	177.0555	$(M-H)^-$	177.0557	−1.22	$C_{10}H_{10}O_3$	2	3-Methoxycinnamic acid	89.0240; 103.3856; 133.0685	Pubchem ID: 637668	8	4.75 ± 4.09
25	19.96	311.2219	$(M-H)^-$	311.2228	−2.77	$C_{18}H_{32}O_4$	2	8,13-Dihydroxy-9,11-octadecadienoic acid	249.2194	Pubchem ID: 5282963	4	7.50 ± 3.28
Average												2.62 ± 1.91

n: number of volunteers in whom the metabolite appears after ingestion of the *S. marianum* encapsulate; RT: retention time; T_{max}: time required to reach the relative maximum plasma level (h); values represent mean ± standard deviation (*n* = number of volunteers in whom the metabolite appears) [a] Database or bibliography used for compound annotation. [b] Mass fragmentation spectrum of the analytical standard in Fig. S2.†

The main phenolic compounds found in the original SM extract administered to the volunteers include silybin, or any of its isomers such as silychristin, silydianin, isosylibin A, isosylibin B.[14] However, upon observing the presence of metabolites in plasma, it became apparent that these compounds did not appear in their intact form in plasma. Instead, they underwent metabolic transformations. In fact, five isomers of silybin glucuronide, two isomers of silybin sulphate, two isomers of silybin sulphate glucuronide, and three isomers of silybin 3,23-bishemisuccinate were detected. It should be noted that the glucuronidated and sulphated forms of silybin found can be either silybin or any of the isomers silychristin, silydianin, isosylibin A, isosylibin B.[14]

Examining the T_{max} values of the silybin glucuronide isomers, differences in T_{max} values were detected since three isomers exhibit T_{max} values between 1.5 and 2 hours, while the other two showed values around 4.5 and 8.5 h, respectively. These variations in T_{max} values could stem from the specific silybin isomer conjugated to glucuronide. However, the limitation of untargeted metabolomics using HPLC-ESI-QTOF-MS lies in determining the exact isomer. It is plausible that certain silybin isomers are absorbed more rapidly, allowing for earlier conjugation. This hypothesis finds support in the findings of Marhol *et al.* (2015), who compared the absorption profiles of different silybin isomers in rats. For instance, they reported a T_{max} of 4.1 hours for silybin A in its free form, whereas for silybin B, it was 1.0 hour.[31] Another explanation could be the site of glucuronidation, as glucuronidation enzymes are expressed in both the liver and small intestine.[32] Studies conducted on rats indicated that isoflavones exhibited slower intestinal glucuronidation compared to hepatic glucuronidation.[33]

In the case of silybin sulphate glucuronide, one of the isomers exhibits a T_{max} of 2.17 ± 0.90, while the other shows a T_{max} of 4.00 ± 2.62. This variation could be attributed to the factors discussed previously for the silybin glucuronide results.

Another compound present in the extract and detected in plasma is taxifolin (dihydroquercetin). Besides being found in its native form in plasma, it also appears with various metabolic phase II transformations or conjugations. These include taxifolin sulphate, methyltaxifolin, and methyltaxifolin glucuronide.

These data agree with the study by Lakeev *et al.* (2023), where they evaluated the metabolism and bioavailability of taxifolin in rats, obtaining T_{max} values of 0.20 ± 0.14 for free taxifolin, 0.12 ± 0.09 for taxifolin sulphate, 0.18 ± 0.12 for methyltaxifolin, and 1.61 ± 1.4 for methyltaxifolin glucuronide, in which the times are shorter due to being rats but appear at early maximum metabolization times, suggesting the rapid metabolization of these compounds.[39]

There are other metabolites present in plasma such as 2-*o*-caffeoylhydroxycitric acid, quercetin glucuronide or eriodictyol, whose presence is due to different reasons. The presence of 2-*o*-caffeoylhydroxycitric acid in plasma may be attributed to the chlorogenic acid content in the original extract. Chlorogenic acid consists of an ester of caffeic acid and quinic acid, and 2-*o*-caffeoylhydroxycitric acid could arise from the degradation of chlorogenic acid. Previous studies have shown that when the original extract contains chlorogenic acid, this compound appears in plasma after ingestion.[40,41] The importance of using untargeted metabolomics strategies to search for metabolites that are not easily predictable to appear in this matrix should be emphasised based on these results.

The presence of quercetin glucuronide in plasma can be attributed to the presence of dihydroquercetin (taxifolin) in the extract and in plasma samples. Dihydroquercetin can undergo reduction to yield quercetin, which is subsequently glucuronidated to form quercetin glucuronide. And lastly, the presence of eriodictyol can be attributed to its presence in the ingested extract, allowing it to pass into plasma in its native form.

3.3.3 Circulating metabolites detected in plasma related to the intake of *Theobroma cacao* extract. Table 3 provides a detailed compilation of 3 annotated metabolites detected in plasma *via* an untargeted metabolomics approach in participants who ingested *T. cacao* extract. Vanillic acid sulphate and trihydroxyoctadecenoic acid were annotated at level 2, while Artonin C was annotated at level 3.

In contrast to the metabolites identified in the ingestion of the two other plant matrices discussed previously, the presence of metabolites following the consumption of *T. cacao* extract is notably lower, with the majority remaining unknown (Table S1†). Although these are unknown compounds, this could be considered a future potential advantage of untargeted metabolomics strategies, as they allow us to detect signals related to supplement intake, which would be undetectable by a targeted approach. It is hoped that with the progress of analytical techniques or the expansion of databases these unknowns can be annotated in the future.

The presence of certain metabolites in plasma stands out, such as vanillic acid sulphate, whose appearance can be attributed to the presence of vanillic acid in the original extract consumed by the volunteers. Additionally, the detection of trihydroxyoctadecenoic acid is noteworthy, as it arises from the metabolism of linolenic acid, a fatty acid present in the ingested extract, catalysed by the microbiota.[42]

The low metabolite content observed in the plasma of volunteers who ingested the TC extract could be attributed to the insufficient richness in phenolic compounds in the extract. The main metabolites that appear in plasma in most previous studies on the bioavailability of cocoa consumption are the flavan-3-ols catechin and epicatechin, or their conjugated forms,[43–45] however, in our study we have not been able to identify these compounds in plasma. This may be due to the fact that the original extract used in our study was not sufficiently rich in these flavan-3-ol compounds. In order to verify this hypothesis, these flavan-3-ols present in the TC extract were quantified (see the ESI† for the specific details of this quantification). Based on the results of this quantification, it is estimated that each volunteer ingested approximately 0.09 mg and 0.98 mg of catechin and epicatechin, respectively, from the 500 mg capsule of extract.

Table 3 HPLC-ESI-QTOF-MS identification information and relative nutrikinetic parameters of the metabolites detected in plasma samples after intake of an extract of *T. cacao*

Peak	RT (min)	Observed *m/z*	Adduct	Theoretical *m/z*	Mass error (ppm)	Molecular formula	Level of annotation	Proposed compound	MS/MS fragments	Ref.[a]	*n*	T_{max}
1	11.66	246.9914	$(M-H)^-$	246.9918	−1.71	$C_8H_8O_7S$	2	Vanillic acid sulphate	167.0365	HMDB0041788	6	1.00 ± 0.00
2	17.36	329.2334	$(M-H)^-$	329.2333	0.03	$C_{18}H_{34}O_5$	2	Trihydroxyoctadecenoic acid	211.1347; 139.2686	48	4	7.63 ± 4.11
3	21.55	677.2423	$(M-H)^-$	677.2392	4.47	$C_{40}H_{38}O_{10}$	3	Artonin C	—	C00008079	4	2.50 ± 2.06
Average												3.71 ± 2.84

n: number of volunteers in whom the metabolite appears after ingestion of the *T. cacao* encapsulate; RT: retention time; T_{max}: time required to reach the relative maximum plasma level (h); values represent mean ± standard deviation (*n* = number of volunteers in whom the metabolite appears). [a]Database or bibliography used for compound annotation.

These compound quantities are significantly lower compared to those consumed in previous reported studies where these bioavailable compounds have been detected in plasma. For example, Ostertag *et al.* (2012) evaluated the bioavailability of these compounds from flavan-3-ol-enriched dark and standard dark chocolates in a total of 42 healthy subjects.[43] They found that both compounds were bioavailable in plasma after the ingestion of 60 g of either flavan-3-ol enriched dark or standard dark chocolate, with levels significatively higher after consuming the enriched one. The amounts ingested of epicatechin and catechin were 257 mg and 53.6 mg for the flavan-3-ol-enriched chocolate, and 84.1 mg and 25.8 mg for the standard dark chocolate, respectively. Thus, it is evident that these values are much higher than those ingested from the extract capsule in our study, which may explain the absence of these metabolites in the plasma samples. Glucuronidated and sulphonated derivatives of these compounds were also detected in plasma in another example reported by Tomas-Barberán *et al.* (2007), who formulated a flavonoid-enriched cocoa powder and conducted a human trial, administering 196.1 mg of epicatechin and 53.3 mg of catechin. Following the consumption of the flavonoid-enriched cocoa, metabolites such as epicatechin glucuronide and epicatechin sulphate were detected in plasma. In the same study, after the administration of conventional cocoa containing 39.6 mg of epicatechin and 24.2 mg of catechin, no sulphated epicatechin was detected in plasma, and the level of glucuronidated epicatechin was five times lower compared to that after consumption of the enriched cocoa. Therefore, this study illustrates that the quantity of ingested flavan-3-ols determines the presence and concentration of the resulting metabolites.[44] Another study by Gómez-Juaristi *et al.* (2019) examined the presence of catechin and epicatechin phase II derivatives in plasma after the consumption of two soluble cocoa products (15 or 25 g of a conventional or a flavanol-rich product, respectively, dissolved in 200 ml of milk). The presence of these metabolites in plasma was attributed to the consumption of 8.55 mg of epicatechin and 4.8 mg of catechin from the conventional drink, while the enriched drink resulted in a total intake of 28.75 mg of epicatechin and 13.25 mg of catechin. These values show clearly that the amounts ingested in our study are much lower in comparison, suggesting a possible reason for why these derivatives compounds were not detected bioavailable in plasma.[45]

Furthermore, the format of cocoa consumption in our study (extract) may have influenced flavan-3-ol bioavailability. Schramm *et al.* (2003) investigated the impact of co-administered foods on catechin and epicatechin absorption from cocoa, demonstrating that concurrent ingestion of bread, sugar, or grapefruit juice affected human bioavailability. Notably, carbohydrate-rich foods significantly increased plasma flavanol levels.[46] Consequently, most cocoa bioavailability studies in the literature utilise cocoa in the form of chocolate, incorporating it within a matrix that includes carbohydrates such as sugar.[47]

Therefore, the fact of not having used an extract rich in flavan-3-ols in this intervention study could be the main

reason for having detected so few bioavailable compounds for TC. This may be also in line with the fact that untargeted methods have limited sensitivity, meaning that compounds present in very low concentrations cannot be detected. In this context, it is evident that despite the great advantages of untargeted methods such as the detection of unexpected compounds or the simultaneous application to bioavailability studies of multiple matrices, there are also limitations. All this suggests that future studies should be carried out with extracts enriched in phenolic compounds to increase the probabilities of detecting bioavailable compounds through untargeted methods.

4 Conclusion

This study highlights the potential of untargeted metabolomics for rapid and comprehensive analysis in biological samples of a wide variety of bioavailable or metabolized exogenous compounds derived from the ingestion of different bioactive plant sources.

This untargeted approach enables a visual assessment and comprehensive analysis of biological samples, providing an initial indication of whether further identification is necessary and identifying the samples along the nutrikinetics that are most significant. This approach has been tested with three different matrices (HS, SM and TC) resulting in the annotation of the main metabolites that appear bioavailable after ingestion of the three matrices in an acute assay in humans. It should be noted that some metabolites such as 2-*o*-caffeoylhydroxycitric acid, quercetin glucuronide or eriodictyol that appear in plasma after SM ingestion could hardly have been obtained by a targeted approach. Thus, this study has been able to annotate the main metabolites without the need to predict the possible routes of metabolism prior to analysis as would have been necessary in a targeted study. Additionally, for a more in-depth analysis, it facilitates the selection of samples for a targeted metabolomics approach, which complements the information obtained.

In this sense, with this research we have proven the potential, but also the limitations, of using this type of untargeted method for bioavailability studies. In fact, we have discovered how the type of bioactive matrix influences the number of metabolites detected by the untargeted method.

Author contributions

María del Carmen Villegas-Aguilar: conceptualization, methodology, investigation, data curation, formal analysis, writing – original draft. María de la Luz Cádiz Gurrea: conceptualization, methodology, formal analysis, supervision. María Herranz-López: methodology, investigation, data curation. Enrique Barrajón-Catalán: conceptualization, methodology, resources, supervision, project administration, funding acquisition, writing – review & editing. David Arráez-Román: resources, project administration, funding acquisition. Álvaro Fernández-Ochoa: conceptualization, methodology, investigation, software, formal analysis, writing – review & editing, supervision, Antonio Segura-Carretero: conceptualization, resources, supervision, project administration, funding acquisition.

Data availability

The data supporting this article have been included as part of the ESI.†

Conflicts of interest

There are no conflicts to declare.

Acknowledgements

This work was supported by the project RTI2018-096724-B-C21 and RTI2018-096724-B-C22 PID2021-125188OB-C31, PID2021-125188OB-C32, TED2021-132043B-I00 and TED2021-129932B-C21 projects funded by MCIN/AEI/10.13039/501100011033/FEDER, UE. This research was also funded by the "Ayudas al funcionamiento de los Grupos operativos de la Asociación Europea para la Innovación (AEI) en materia de productividad y sostenibilidad agrícolas en el sector del olivar, 2020" (grant number GOPO-GR-20-0001), the Generalitat Valenciana (grant number PROMETEO/2021/059) and Agencia Valenciana de la Innovación (grant number INNEST/2022/103). M. d. C. V.-A. thanks her grant FPU19/01146 funded by MCIN/AEI/10.13039/501100011033. M. d. l. L. C.-G. thanks her contract RYC2021-032119-I funded by MCIN/AEI/10.13039/501100011033. M. H.-L. and E. B.-C. were supported by the "Requalification for university teachers grant" from the Spanish Ministry of Universities and European Union Next Generation program.

References

1 M. d. C. Villegas-Aguilar, Á. Fernández-Ochoa, M. d. l. L. Cádiz-Gurrea, S. Pimentel-Moral, J. Lozano-Sánchez, D. Arráez-Román and A. Segura-Carretero, Pleiotropic Biological Effects of Dietary Phenolic Compounds and their Metabolites on Energy Metabolism, Inflammation and Aging, *Molecules*, 2020, **25**, 596.
2 A. Crozier, D. Del Rio and M. N. Clifford, Bioavailability of dietary flavonoids and phenolic compounds, *Mol. Aspects Med.*, 2010, **31**, 446–467.
3 G. R. Velderrain-Rodríguez, H. Palafox-Carlos, A. Wall-Medrano, J. F. Ayala-Zavala, C.-Y. O. Chen, M. Robles-Sánchez, H. Astiazaran-García, E. Alvarez-Parrilla and G. A. González-Aguilar, Phenolic compounds: their journey after intake, *Food Funct.*, 2014, **5**, 189–197.

4 M. Gómez-Juaristi, S. Martínez-López, B. Sarria, L. Bravo and R. Mateos, Absorption and metabolism of yerba mate phenolic compounds in humans, *Food Chem.*, 2018, **240**, 1028–1038.
5 M. Achour, L. Bravo, B. Sarriá, M. Ben Fredj, M. Nouira, A. Mtiraoui, S. Saguem and R. Mateos, Bioavailability and nutrikinetics of rosemary tea phenolic compounds in humans, *Food Res. Int.*, 2021, **139**, 109815.
6 Á. Fernández-Ochoa, M. d. l. L. Cádiz-Gurrea, P. Fernández-Moreno, A. Rojas-García, D. Arráez-Román and A. Segura-Carretero, Recent Analytical Approaches for the Study of Bioavailability and Metabolism of Bioactive Phenolic Compounds, *Molecules*, 2022, **27**(3), 777.
7 S. Piovesana, C. Cavaliere, A. Cerrato, C. M. Montone, A. Laganà and A. L. Capriotti, Developments and pitfalls in the characterization of phenolic compounds in food: From targeted analysis to metabolomics-based approaches, *TrAC, Trends Anal. Chem.*, 2020, **133**, 116083.
8 A. Scalbert, L. Brennan, O. Fiehn, T. Hankemeier, B. S. Kristal, B. van Ommen, E. Pujos-Guillot, E. Verheij, D. Wishart and S. Wopereis, Mass-spectrometry-based metabolomics: limitations and recommendations for future progress with particular focus on nutrition research, *Metabolomics*, 2009, **5**, 435–458.
9 I. Gertsman and B. A. Barshop, Promises and pitfalls of untargeted metabolomics, *J. Inherited Metab. Dis.*, 2018, **41**, 355–366.
10 A. Ribbenstedt, H. Ziarrusta and J. P. Benskin, Development, characterization and comparisons of targeted and non-targeted metabolomics methods, *PLoS One*, 2018, **13**, e0207082.
11 G. Riaz and R. Chopra, A review on phytochemistry and therapeutic uses of Hibiscus sabdariffa L., *Biomed. Pharmacother.*, 2018, **102**, 575–586.
12 N. Vargas-Mendoza, Hepatoprotective effect of silymarin, *World J. Hepatol.*, 2014, **6**, 144.
13 D. L. Pucciarelli and L. E. Grivetti, The Medicinal Use of Chocolate in Early North America, *Mol. Nutr. Food Res.*, 2008, **52**, 1215–1227.
14 M. d. C. Villegas-Aguilar, N. Sánchez-Marzo, Á. Fernández-Ochoa, C. Del Río, J. Montaner, V. Micol, M. Herranz-López, E. Barrajón-Catalán, D. Arráez-Román, M. d. l. L. Cádiz-Gurrea and A. Segura-Carretero, Evaluation of Bioactive Effects of Five Plant Extracts with Different Phenolic Compositions against Different Therapeutic Targets, *Antioxidants*, 2024, **13**, 217.
15 D. Broadhurst, R. Goodacre, S. N. Reinke, J. Kuligowski, I. D. Wilson, M. R. Lewis and W. B. Dunn, Guidelines and considerations for the use of system suitability and quality control samples in mass spectrometry assays applied in untargeted clinical metabolomic studies, *Metabolomics*, 2018, **14**, 72.
16 Á. Fernández-Ochoa, R. Quirantes-Piné, I. Borrás-Linares, M. d. l. L. Cádiz-Gurrea, M. E. Alarcón Riquelme, C. Brunius and A. Segura-Carretero, A Case Report of Switching from Specific Vendor-Based to R-Based Pipelines for Untargeted LC-MS Metabolomics, *Metabolites*, 2020 **10**, 28.
17 C. Brunius, L. Shi and R. Landberg, Large-scale untargeted LC-MS metabolomics data correction using between-batch feature alignment and cluster-based within-batch signal intensity drift correction, *Metabolomics*, 2016, **12**, 173.
18 Y. Zhang, M. Huo, J. Zhou and S. Xie, PKSolver: An add-in program for pharmacokinetic and pharmacodynamic data analysis in Microsoft Excel, *Comput. Methods Programs Biomed.*, 2010, **99**, 306–314.
19 A. Gil de la Fuente, J. Godzien, M. Fernández López, F. J. Rupérez, C. Barbas and A. Otero, Knowledge-based metabolite annotation tool: CEU Mass Mediator, *J. Pharm. Biomed. Anal.*, 2018, **154**, 138–149.
20 L. W. Sumner, A. Amberg, D. Barrett, M. H. Beale, R. Beger, C. A. Daykin, T. W.-M. Fan, O. Fiehn, R. Goodacre, J. L. Griffin, T. Hankemeier, N. Hardy, J. Harnly, R. Higashi, J. Kopka, A. N. Lane, J. C. Lindon, P. Marriott, A. W. Nicholls, M. D. Reily, J. J. Thaden and M. R. Viant, Proposed minimum reporting standards for chemical analysis, *Metabolomics*, 2007, **3**, 211–221.
21 H. Gowda, J. Ivanisevic, C. H. Johnson, M. E. Kurczy, H. P. Benton, D. Rinehart, T. Nguyen, J. Ray, J. Kuehl, B. Arevalo, P. D. Westenskow, J. Wang, A. P. Arkin, A. M. Deutschbauer, G. J. Patti and G. Siuzdak, Interactive XCMS Online: Simplifying Advanced Metabolomic Data Processing and Subsequent Statistical Analyses, *Anal. Chem.*, 2014, **86**, 6931–6939.
22 T. Lippolis, M. Cofano, G. R. Caponio, V. De Nunzio and M. Notarnicola, Bioaccessibility and Bioavailability of Diet Polyphenols and Their Modulation of Gut Microbiota, *Int. J. Mol. Sci.*, 2023, **24**, 3813.
23 J. Izquierdo-Vega, D. Arteaga-Badillo, M. Sánchez-Gutiérrez, J. Morales-González, N. Vargas-Mendoza, C. Gómez-Aldapa, J. Castro-Rosas, L. Delgado-Olivares, E. Madrigal-Bujaidar and E. Madrigal-Santillán, Organic Acids from Roselle (Hibiscus sabdariffa L.)—A Brief Review of Its Pharmacological Effects, *Biomedicines*, 2020, **8**, 100.
24 S. A. Heleno, A. Martins, M. J. R. P. Queiroz and I. C. F. R. Ferreira, Bioactivity of phenolic acids: Metabolites versus parent compounds: A review, *Food Chem.*, 2015, **173**, 501–513.
25 A. Arce-Reynoso, R. Mateos, E. J. Mendivil, V. M. Zamora-Gasga and S. G. Sáyago-Ayerdi, Bioavailability of bioactive compounds in Hibiscus sabdariffa beverage as a potential anti-inflammatory, *Food Res. Int.*, 2023, **174**, 113581.
26 P. K. Tyagi and S. Tyagi, Evaluation of Ascorbic acid contents in Hibiscus rosa-sinensis flowers and Citrus sinensis fruits, *Res. J. Pharm., Biol. Chem. Sci.*, 2018, **9**, 67–70.
27 A. M. Duarte, M. P. Guarino, S. Barroso and M. M. Gil, Phytopharmacological Strategies in the Management of Type 2 Diabetes Mellitus, *Foods*, 2020, **9**(3), 271.
28 E. Avalos-Martínez, J. A. Pino, S. Sáyago-Ayerdi, O. Sosa-Moguel and L. Cuevas-Glory, Assessment of volatile compounds and sensory characteristics of Mexican hibiscus

(Hibiscus sabdariffa L.) calyces hot beverages, *J. Food Sci. Technol.*, 2019, **56**, 360–366.

29 D. Amaya-Cruz, I. F. Peréz-Ramírez, J. Pérez-Jiménez, G. M. Nava and R. Reynoso-Camacho, Comparison of the bioactive potential of Roselle (Hibiscus sabdariffa L.) calyx and its by-product: Phenolic characterization by UPLC-QTOF MS and their anti-obesity effect in vivo, *Food Res. Int.*, 2019, **126**, 108589.

30 S. Pimentel-Moral, I. Borrás-Linares, J. Lozano-Sánchez, D. Arráez-Román, A. Martínez-Férez and A. Segura-Carretero, Microwave-assisted extraction for Hibiscus sabdariffa bioactive compounds, *J. Pharm. Biomed. Anal.*, 2018, **156**, 313–322.

31 P. Marhol, P. Bednář, P. Kolářová, R. Večeřa, J. Ulrichová, E. Tesařová, E. Vavříková, M. Kuzma and V. Křen, Pharmacokinetics of pure silybin diastereoisomers and identification of their metabolites in rat plasma, *J. Funct. Foods*, 2015, **14**, 570–580.

32 J. P. E. Spencer, G. Chowrimootoo, R. Choudhury, E. S. Debnam, S. K. Srai and C. Rice-Evans, The small intestine can both absorb and glucuronidate luminal flavonoids, *FEBS Lett.*, 1999, **458**, 224–230.

33 J. Chen, S. Wang, X. Jia, S. Bajimaya, H. Lin, V. H. Tam and M. Hu, Disposition of flavonoids via recycling: comparison of intestinal versus hepatic disposition., *Drug Metab. Dispos.*, 2005, **33**, 1777–1784.

34 M. Umair, T. Sultana, Z. Xiaoyu, A. M. Senan, S. Jabbar, L. Khan, M. Abid, M. A. Murtaza, D. Kuldeep, N. A. S. Al-Areqi and L. Zhaoxin, LC–ESI–QTOF/MS characterization of antimicrobial compounds with their action mode extracted from vine tea (*Ampelopsis grossedentata*) leaves, *Food Sci. Nutr.*, 2022, **10**, 422–435.

35 P. Yang, F. Xu, H.-F. Li, Y. Wang, F.-C. Li, M.-Y. Shang, G.-X. Liu, X. Wang and S.-Q. Cai, Detection of 191 Taxifolin Metabolites and Their Distribution in Rats Using HPLC-ESI-IT-TOF-MSn, *Molecules*, 2016, **21**, 1209.

36 K. Valentová, J. Havlík, P. Kosina, B. Papoušková, J. D. Jaimes, K. Káňová, L. Petrásková, J. Ulrichová and V. Křen, Biotransformation of Silymarin Flavonolignans by Human Fecal Microbiota, *Metabolites*, 2020, **10**, 29.

37 J. Vrba, B. Papoušková, L. Roubalová, M. Zatloukalová, D. Biedermann, V. Křen, K. Valentová, J. Ulrichová and J. Vacek, Metabolism of flavonolignans in human hepatocytes, *J. Pharm. Biomed. Anal.*, 2018, **152**, 94–101.

38 D. Biedermann, E. Vavříková, L. Cvak and V. Křen, Chemistry of silybin, *Nat. Prod. Rep.*, 2014, **31**, 1138–1157.

39 A. P. Lakeev, E. A. Yanovskaya, V. A. Yanovsky, G. A. Frelikh and M. O. Andropov, Novel aspects of taxifolin pharmacokinetics: Dose proportionality, cumulative effect, metabolism, microemulsion dosage forms, *J. Pharm. Biomed. Anal.*, 2023, **236**, 115744.

40 Z. Liao, S. Zhang, W. Liu, B. Zou, L. Lin, M. Chen, D. Liu, M. Wang, L. Li, Y. Cai, Q. Liao and Z. Xie, LC-MS-based metabolomics analysis of Berberine treatment in ulcerative colitis rats, *J. Chromatogr. B: Anal. Technol. Biomed. Life Sci.*, 2019, **1133**, 121848.

41 S. G. Sáyago-Ayerdi, K. Venema, M. Tabernero, B. Sarriá, L. Bravo and R. Mateos, Bioconversion of polyphenols and organic acids by gut microbiota of predigested Hibiscus sabdariffa L. calyces and Agave (A. tequilana Weber) fructans assessed in a dynamic in vitro model (TIM-2) of the human colon, *Food Res. Int.*, 2021, **143**, 110301.

42 C. T. Hou, W. Brown, D. P. Labeda, T. P. Abbott and D. Weisleder, Microbial production of a novel trihydroxy unsaturated fatty acid from linoleic acid, *J. Ind. Microbiol. Biotechnol.*, 1997, **19**, 34–38.

43 L. M. Ostertag, P. A. Kroon, S. Wood, G. W. Horgan, E. Cienfuegos-Jovellanos, S. Saha, G. G. Duthie and B. de Roos, Flavan–3–ol–enriched dark chocolate and white chocolate improve acute measures of platelet function in a gender–specific way—a randomized–controlled human intervention trial, *Mol. Nutr. Food Res.*, 2013, **57**, 191–202.

44 F. A. Tomas-Barberán, E. Cienfuegos-Jovellanos, A. Marín, B. Muguerza, A. Gil-Izquierdo, B. Cerdá, P. Zafrilla, J. Morillas, J. Mulero, A. Ibarra, M. A. Pasamar, D. Ramón and J. C. Espín, A New Process To Develop a Cocoa Powder with Higher Flavonoid Monomer Content and Enhanced Bioavailability in Healthy Humans, *J. Agric. Food Chem.*, 2007, **55**, 3926–3935.

45 M. Gómez-Juaristi, B. Sarria, S. Martínez-López, L. Bravo-Clemente and R. Mateos, Flavanol Bioavailability in Two Cocoa Products with Different Phenolic Content. A Comparative Study in Humans, *Nutrients*, 2019, **11**, 1441.

46 D. D. Schramm, M. Karim, H. R. Schrader, R. R. Holt, N. J. Kirkpatrick, J. A. Polagruto, J. L. Ensunsa, H. H. Schmitz and C. L. Keen, Food effects on the absorption and pharmacokinetics of cocoa flavanols, *Life Sci.*, 2003, **73**, 857–869.

47 J. Oracz, E. Nebesny, D. Zyzelewicz, G. Budryn and B. Luzak, Bioavailability and metabolism of selected cocoa bioactive compounds: A comprehensive review, *Crit. Rev. Food Sci. Nutr.*, 2020, **60**, 1947–1985.

48 G. Vargas-Arana, C. Merino-Zegarra, M. Tang, M. W. Pertino and M. J. Simirgiotis, UHPLC–MS Characterization, and Antioxidant and Nutritional Analysis of Cocoa Waste Flours from the Peruvian Amazon, *Antioxidants*, 2022, **11**, 595.

